

# A Generic Feasibility Study of Batch Reactive Distillation in Hybrid Configurations

C. Stéger, T. Lukács, and E. Rév

Dept. of Chemical and Environmental Process Engineering, Budapest University of Technology and Economics,  
1521 Budapest, Hungary

M. Meyer

Ecole Nationale Supérieure d'Ingénieurs en Arts Chimiques et Technologiques, Laboratoire de Génie Chimique,  
UMR CNRS 5503, ENSIACET-UPS-CNRS, BP 1301, 5 rue Paulin Talabot, 31106 Toulouse, France

Z. Lelkes

Dept. of Chemical and Environmental Process Engineering, Budapest University of Technology and Economics,  
1521 Budapest, Hungary

DOI 10.1002/aic.11731

Published online April 8, 2009 in Wiley InterScience (www.interscience.wiley.com).

*A new graphical feasibility method is developed to investigate batch reactive distillation processes in middle vessel column. The suggested methodology can deal with fully reactive, nonreactive, and complex column configuration. A new formulation is suggested to describe the composition profiles in the reactive sections. Its application has made possible to develop a generic feasibility methodology containing the same model equations independently of the presence or absence of reaction. By combining the reactive and nonreactive models, not only the fully reactive and fully nonreactive but also hybrid configurations can be studied. Feasibility criteria related to the hybrid configurations are also presented. Application of the new methodology is demonstrated on the production of ethyl acetate in batch reactive distillation. Five configurations are found feasible; pure EtOAc is produced as distillate, and pure H<sub>2</sub>O is produced at the bottom. In each case, continuous feeding of AcOH is necessary. © 2009 American Institute of Chemical Engineers AIChE J, 55: 1185–1199, 2009*

**Keywords:** separation, reactive distillation, design, feasibility study, hybrid column

## Introduction

Applying reactive distillation is one of the most important options for process intensification.<sup>1,2</sup> In traditional processes, the reaction itself and the separation of the reaction products are carried out in subsequent operations, and in separate devices. Total conversion cannot be reached if the reaction is equilibrium limited, and the nonreacted components must be recycled to the reactor. This recycling increases the

investment and the energy demand, as well. In addition, transportation of the compounds between the equipment units makes the production more hazardous.

In reactive distillation, on the other hand, the reaction and the separation are carried out in one operation, in the same unit (Figure 1). The investment costs are decreased because of the decreasing number of operation units. The operation costs, the hazards related to the process, and the amount of by-products are also decreased because no external recycling is applied.

In spite of the numerous advantages, the number of industrial applications is yet small. One of the reasons of this reluctance may be the lack of well-known design and control

Correspondence concerning this article should be addressed to C. Stéger at stegercsaba@gmail.com.

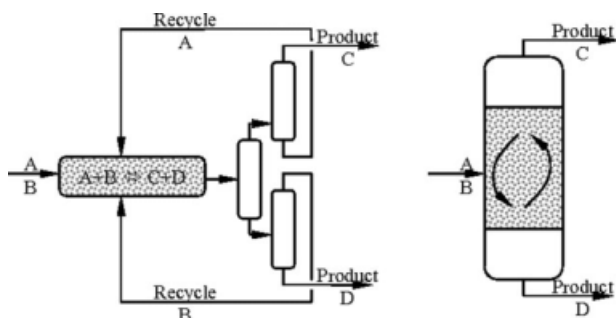


**Figure 1. Schemes of the traditional reaction/separation and the reactive distillation processes.**

methodology. Hence, the thorough investigation and deep understanding of this integrated process is a really important task.

Preliminary design methodologies are normally applied to find a feasible configuration accompanied by a suggested value or range of the most important operation parameters. These methods usually rely on some simplified model with thermodynamic approach,<sup>3</sup> namely they neglect such technical parameters such as the hold-up, the pressure drop, the height and the diameter of the column, and so forth. Most of the preliminary methods work in graphical mode; this eases their understanding but, at the same time, limits their applicability. The graphical methods without any modification cannot be applied over 3D.

The design methodologies of the conventional and the extractive distillation are well elaborated for both continuous and batch processes.<sup>4-6</sup> Feasibility studies for batch reactive distillations have been performed with nonreactive columns attached to a reactive reboiler or stripper,<sup>7-9</sup> but the set of possible configurations is wider if the hybrid configurations are also taken into account.

To get a generic view about the feasibility of a process, most of the possible configurations (in principle an infinite number) must be investigated. They can either be studied one-by-one with unique feasibility studies or simultaneously with a generic feasibility method that permits the investigation of all the configurations together. Figure 2 shows all the possible configurations of batch rectifier with reactive still

(boiler) and at most one feed. Our aim here is to present a generic feasibility study that is able to investigate simultaneously all the column configurations in Figure 2, together with their analogues for the batch stripper configurations, and their extensions for the batch middle vessel (MVC) configurations, which are combinations of batch rectifier and batch stripper.

To investigate a hybrid configuration, a feasibility methodology should be able to predict the column profiles in reactive and nonreactive column sections with and without additional feed, and should be able to investigate the contact points of the different column sections. Some of the published methodologies have already proposed methodologies for particular cases, but their application is limited. Either their assumptions are too strict,<sup>10</sup> or they can be used for staged columns only,<sup>11-14</sup> or the methodology cannot predict the composition profile in an extractive section<sup>15,16</sup>.

According to Pisarenko et al.,<sup>10</sup> the presence of a reaction does not affect the composition profile; thus, the reactive profiles can be predicted with computing the nonreactive ones. Using a reactive section is necessary if the material balance of the distillation column crosses the reactive domain and the reactive composition profile takes place in the forward reaction zone. The assumptions taken into account by Pisarenko et al.,<sup>10</sup> are invalid because the presence of the reaction can change the composition profile significantly.

Dragomir and Jobson<sup>14</sup> deal with the conceptual design of continuous one-feed hybrid column configurations. The published design method is based on the stage composition lines<sup>13</sup> (SCL). SCLs can be applied to predict the compositions of a specific tray for different reflux or reboil ratios. To calculate the SCLs, the same equations can be used as for the distillation lines (DL<sup>16</sup>), but the role of the fixed and the free parameters are reversed. During a study based on DLs, the fixed parameter is the reflux ratio ( $R$ ) in the rectifying section and the reboil ratio ( $S$ ) in the stripping section, whereas the free parameter is the number of theoretical stages. In the case of a study based on SCLs, just the contrary, the number of theoretical stages is fixed in both sections, and the values of  $R$  and  $S$  are varied. The feasibility condition of the SCLs is the same as that of the DLs, namely, the intersection of the two segments of the profile.

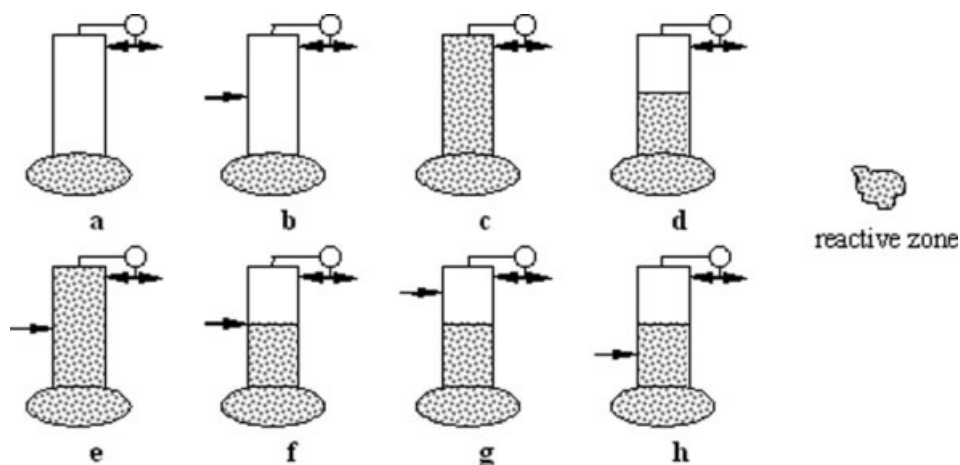


**Figure 2. Batch reactive distillation configurations in rectifier with a maximum of one feed.**

Because stage profiles are calculated, the feasibility condition must be specified for continuous profiles.

Bessling et al.<sup>16</sup> used the DLs for studying double-feed distillation columns, but only the composition profiles in the stripping and in the rectifying sections were calculated. The necessity of a middle section, that is, a second feed, is predicted in the case of a product being a saddle. In the spirit of Bessling et al.,<sup>16</sup> use of a hybrid configuration is necessary if the product is situated outside the reactive space. A drawback of this methodology, in spite of its really important statements, is that the evaluation of the composition profile in the middle section can be visualized after several simulation runs only; thus, the determination of the proper operation parameters  $R$ ,  $S$ , and the ratio of the two feed flow rates, is very difficult.

Chin et al.<sup>15</sup> also studied the double-feed reactive distillation columns, without calculating the composition profile in the middle section. The composition profile between the two feeds is merely estimated. Instead of the whole composition profile in the middle section, only its initial direction is calculated, and used for estimating the profile. It is not evident that the obtained "critical composition region" (CCR) really means an unfeasible region for the middle section.

Boneta et al.<sup>17</sup> studied the combination of reactive distillation and pressure swing distillation for the transesterification between methyl-acetate and ethyl-acetate. This study was performed with the analysis of the reactive residue curve maps, and of the DLs calculated at finite reflux ratio.

Although the methodologies in the quoted papers can be applied for selected case studies only, all of them contain some sort of information that can be used to formulate a general approach. We have applied the results of the cited articles in creating our generic feasibility methodology for hybrid configurations of batch reactive distillation. With some modifications, the suggested methodology can be extended to continuous processes, as well.

In this article, the generic feasibility methodology of batch reactive distillation with reactions in chemical equilibrium is first presented in details, and then the proposed method is applied to the production of ethyl acetate in a batch reactive distillation column.

## Generic Feasibility Study

The following basic notions and assumptions are applied in the following feasibility study.

A batch separation process is called feasible if, starting from the initial charge, the desired product(s) can be withdrawn. The desired product is the distillate in the case of a batch rectifier, the bottom product in the case of a batch stripper, and both distillate and bottom products in the case of a middle vessel column operated batchwise. In these cases, we speak about feasible separation or feasible process.

Destination region is a narrow interval containing only and all the possible compositions of the product(s) of which the purity is not less than desired.

The commonly used simplifying assumptions are applied in our feasibility methodology. One instantaneously equilibrium limited reaction is present in the liquid phase. The reaction heat, the influence of the catalyst on the instantaneous vapor-liquid equilibrium (VLE), and the liquid hold-up are neglected. Constant molar overflow is assumed.

The main elements of the feasibility methodology are (1) the column section profiles, (2) the still path, and (3) the composition pairs formed at the column section borders.

Because the column profile informs us about the compositions in the column, and so about the product composition, it must be calculated. The column profile consists of column section profiles and possible sudden composition jumps at the section borders.

The main vessel of a device is either the reboiler, the reflux drum, or the middle vessel (MV) depending on if a batch rectifier, a batch stripper, or a batch MVC is applied, respectively. Because the composition in the main vessel changes in time, the movement of this composition must also be predicted. The trace of this composition is called still-path, irrespective to whether the main vessel is the reflux drum, the middle vessel, or the boiler at the bottom.

A column configuration might consist of several column sections, and the feasibility may depend on the composition pairs at their junctions. Therefore, these composition pairs must also be investigated in a generic feasibility study. Such composition pairs may form a single composition if the two column section profiles intersect, but such an intersection is not always necessary if reaction is also involved. For brevity, we generally speak about junction points when such intersections or composition pairs are mentioned.

## Column profiles

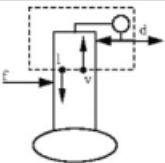
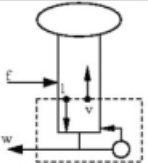
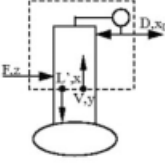
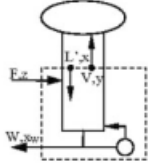
To have a generic feasibility methodology, the model equations of the nonreactive and reactive sections should be written in the same mathematical form because they should represent the same way of thinking. The model equations can be constructed from a submodel related to batch rectifiers and a separate submodel related to batch strippers. Our research group has already published the model equations for nonreactive batch extractive distillation performed in batch rectifier<sup>4</sup> and in batch stripper.<sup>18</sup> Table 1 summarizes all the model equations for nonreactive column profiles. The differential equation describing the liquid component flow rate is of the same mathematical form in each column section, but the operating line equation expressing the vapor component flow rate at the same column level is varied in the system according to the actual column section. The differential equation (see in the Table 1) of this widely used and referred model<sup>19–24</sup> is based on the driving force of the distillation, namely the concentration difference between the real vapor mole fraction  $y_i$  and the one in equilibrium with the liquid phase ( $y_i^*$ ). These mole fractions multiplied with the common total vapor flow rate give the component flow rates at the right hand side of Eq. 2.

According to Doherty and Buzad,<sup>1</sup> the column profiles can be represented in transformed space in the case of instantaneously equilibrium limited reactions. The transformation suggested by Doherty and Buzad<sup>1</sup> is really useful because nearly all the relations of nonreactive distillation (operating lines, mass balances, etc.) remain in the same form after applying the transformation<sup>11,12</sup>:

$$x_i = \frac{x_i - \frac{v_i}{v_{\text{ref}}} \cdot x_{\text{ref}}}{1 - \frac{v_i}{v_{\text{ref}}} \cdot x_{\text{ref}}} \quad \text{and} \quad Y_i = \frac{y_i - \frac{v_i}{v_{\text{ref}}} \cdot y_{\text{ref}}}{1 - \frac{v_i}{v_{\text{ref}}} \cdot y_{\text{ref}}} \quad (1)$$

All the publications about reactive distillation with instantaneously equilibrium limited reactions use transformed mole fractions and transformed total flow rates. These transformations can be used to model reactive sections, but cannot be

**Table 1. Model Equations of the Nonreactive Column Sections**

	non reactive batch rectifier [4]	non reactive batch stripper [17]
section without feed		
	$\frac{dl_i}{dh} = v_i - v_i^*$ (eq. 2)	$\frac{dl_i}{dh} = v_i - v_i^*$ (eq. 2)
	$v_i = l_i + d_i$ (eq. 3)	$v_i = l_i - w_i$ (eq. 4)
section with feed (extractive section)		
	$\frac{dl'_i}{dh} = v_i - v_i^*$ (eq. 2)	$\frac{dl'_i}{dh} = v_i - v_i^*$ (eq. 2)
	$v_i = l'_i + d_i - f_i$ (eq. 5)	$v_i = l'_i - w_i + f_i$ (eq. 6)

directly applied to the modeling equations, collected in Table 1, describing nonreactive sections. The modeling equations have to be formulated to reactive sections, too. The transformation expressed by Eq. 1 transform the mole fractions only, and does not transform the flow rates. Transformations applied to total flow rates does not transform the mole fractions. To obtain an adequate model, applicable to hybrid columns, a new transformation is introduced in this article. Instead of transformed mole fractions and transformed total flow rates, we apply transformed component flow rates. The derived model equations are collected in the Table 2; derivation of the equations is presented in Appendix A.

Transformed mole fractions can be simply calculated from the transformed molar flow rates in the usual way, by normalizing them. The mole fractions calculated this way are equivalent to those calculated with Eq. 1, suggested by Doherty and Buzad.<sup>1</sup> The proof of the equivalence is presented in Appendix B.

### Reactive still path

The hardest task of the feasibility study is computing the still-path. Because the transformed mole fractions are well constrained variables, the column profiles are always represented in mole fractions instead of molar flow rates. To decide whether a separation is feasible or not, the column profiles and the still-path must be represented in the same figure. Thus, the reactive still-path model must be a system of differential equations of the reactive mole fractions.

In the spirit of Espinosa,<sup>11,12</sup> the form of the material balances expressed in reactive mole fractions remains the same in the presence of equimolar or nonequimolar reactions in the case of a steady state system. But this is not so in a dynamic system. The differential equations expressed in mole fractions keep their form in the case of the equimolar

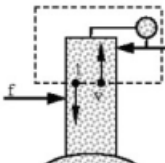
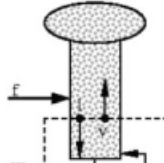
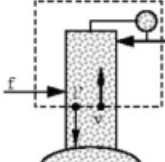
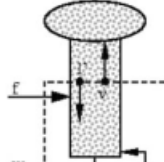
reactions, Eqs. 15 and 17, but not in the case of the nonequimolar reactions, Eq. 16. Table 3 presents the differential equations of the nonreactive and the reactive still-paths for a MVC without feed. The detailed derivation of the reactive still-path is presented in Appendix C.

### Junction points

Four junction points are to be considered: (1) junction of two nonreactive sections, (2) junction of two reactive sections, (3) junction of an upper nonreactive section with a lower reactive section, and finally (4) junction of an upper reactive section with a lower nonreactive section.

The first case, when two nonreactive sections are in contact, has already been investigated in the feasibility method published by Lelkes et al.<sup>4</sup> The feasibility condition is the intersection of the calculated profiles. The same feasibility

**Table 2. Model Equations of the Reactive Column Sections**

	reactive batch rectifier	reactive batch stripper
section without feed		
	$\tilde{l}_i = l_i - \frac{v_i}{v_{ref}} \cdot l'_{ref}$ (eq. 7)	$\tilde{l}_i = l_i - \frac{v_i}{v_{ref}} \cdot l'_{ref}$ (eq. 7)
	$\frac{d\tilde{l}_i}{dh} = \tilde{v}_i - \tilde{v}_i^*$ (eq. 8)	$\frac{d\tilde{l}_i}{dh} = \tilde{v}_i - \tilde{v}_i^*$ (eq. 8)
	$\tilde{v}_i = \tilde{l}_i + \tilde{d}_i$ (eq. 9)	$\tilde{v}_i = \tilde{l}_i - \tilde{w}_i$ (eq. 10)
	$x_i = \frac{l_i}{\sum_{j=1}^{nc} l_j}$ (eq. 11)	$x_i = \frac{l_i}{\sum_{j=1}^{nc} l_j}$ (eq. 11)
	$K = \prod_{j=1}^{nc} x_j^{a_j}$ (eq. 12)	$K = \prod_{j=1}^{nc} x_j^{a_j}$ (eq. 12)
section with feed (extractive section)		
	$\tilde{l}'_i = l'_i - \frac{v_i}{v_{ref}} \cdot l'_{ref}$ (eq. 7)	$\tilde{l}'_i = l'_i - \frac{v_i}{v_{ref}} \cdot l'_{ref}$ (eq. 7)
	$\frac{d\tilde{l}'_i}{dh} = \tilde{v}_i - \tilde{v}_i^*$ (eq. 8)	$\frac{d\tilde{l}'_i}{dh} = \tilde{v}_i - \tilde{v}_i^*$ (eq. 8)
	$\tilde{v}_i = \tilde{l}'_i + \tilde{d}_i - \tilde{f}_i$ (eq. 13)	$\tilde{v}_i = \tilde{l}'_i - \tilde{w}_i + \tilde{f}_i$ (eq. 14)
	$x_i = \frac{l'_i}{\sum_{j=1}^{nc} l'_j}$ (eq. 11)	$x_i = \frac{l'_i}{\sum_{j=1}^{nc} l'_j}$ (eq. 11)
	$K = \prod_{j=1}^{nc} x_j^{a_j}$ (eq. 12)	$K = \prod_{j=1}^{nc} x_j^{a_j}$ (eq. 12)



**Table 3. Model Equations of the Nonreactive and the Reactive Still-Path for MVC**

non reactive [27]	$\frac{dx_{MV,j}}{dt} =$	$D \cdot (x_{MV,j} - x_{D,j}) + W \cdot (x_{MV,j} - x_{W,j})$	(eq. 15)
reactive still-path $v_T \neq 0$	$\dot{U} \cdot \frac{dx_{MV,j}}{dt} =$	$\dot{D} \cdot \left( X_{MV,j} \cdot \frac{1 - \frac{v_T}{v_{ref}} \cdot x_{MV,ref}}{1 - \frac{v_T}{v_{ref}} \cdot x_{D,ref}} - X_{D,j} \right) +$ $+ \dot{W} \cdot \left( X_{MV,j} \cdot \frac{1 - \frac{v_T}{v_{ref}} \cdot x_{MV,ref}}{1 - \frac{v_T}{v_{ref}} \cdot x_{W,ref}} - X_{W,j} \right) -$ $- X_{MV,j} \cdot \left( 1 - \frac{v_T}{v_{ref}} \cdot x_{MV,ref} \right) \cdot v_T \cdot \sum_{\text{column}} \frac{\dot{E}}{v} +$ $+ U_{MV} \cdot X_{MV,j} \cdot \frac{v_T}{v_{ref}} \cdot \frac{dx_{MV,ref}}{dt}$	(eq. 16)
$v_T = 0$	$\frac{dx_{MV,j}}{dt} =$	$D \cdot (x_{MV,j} - x_{D,j}) + W \cdot (x_{MV,j} - x_{W,j})$	(eq. 17)

condition can be applied in the second case, that is, when two reactive sections are in contact. The calculated profiles must cross each other but in this case the intersection must be investigated in the transformed space.

The feasibility condition of the third and the fourth cases, that is, when a reactive section and a nonreactive section are in contact, is created in the spirit of Dragomir and Jobson.<sup>14</sup> According to Dragomir and Jobson,<sup>14</sup> the feasibility condition is the continuity of the liquid and vapor composition profiles in the column. Because in their case, the distillation column contains theoretical stages, all the calculated liquid compositions and the vapor compositions being in VLE with the liquid phase, appear in the column (see Figure 3). Thus, the intersection of the calculated profile satisfies the feasibility condition.

In the case of continuous profiles, the same condition cannot be used without modification because the vapor composition may appear at a higher position of the column than the liquid composition to which it is in equilibrium with. If the same condition is applied then continuity of both profiles cannot be simultaneously maintained (see Figure 4a). To simplify the problem, the junction point between a reactive and a nonreactive section is supposed to be in VLE (see Figure 4b).

The problem occurs only if a reactive section (or vessel) is situated below a nonreactive section. The model equations can be integrated either upward or downward in the column, but in each case, the result is a liquid composition profile. If the integration is done upward (in the stripping part of the column), the feasibility condition remains the same, namely, the calculated composition profiles in the lower and upper sections must cross each other. If the profiles are integrated downward, a dew point profile must also be simultaneously calculated from the vapor compositions of the operating line. For feasible column sections, the dew point profile of the upper section must cross the liquid composition (boiling point) profile of the lower section (see Figure 5).

### Strategy of the feasibility study

In this paragraph, the strategy of a feasibility study is presented step-by-step (Figure 6) applying the elements described in the sections above.

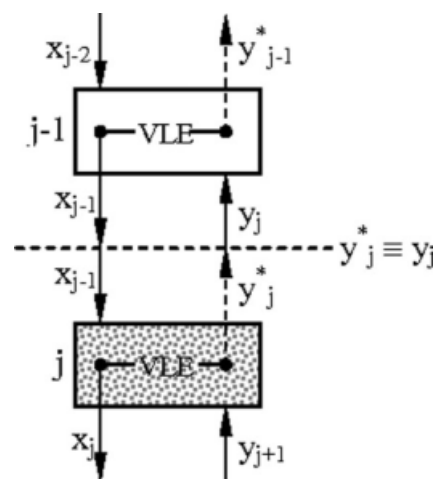


**Figure 3. Continuity condition in the case of theoretical stages.**

Step 0: Before performing a feasibility study, the parameters describing the system ( $K$ ; VLE parameters; etc.), the main specifications ( $p$ ,  $z$ ,  $x_D$ , and  $x_W$  destination regions), and the initial conditions ( $U_{MV}(0)$ ;  $x_{MV}(0)$ ) are given.

Step 1: Parameters ( $R$ ;  $S$ ;  $F$ ), and particular  $x_D$  and  $x_W$  compositions (inside the destination regions) are temporarily specified.

Step 2: Composition profile maps (PMs) are calculated with the same parameters. The PMs in the uppermost and lowest column sections must be distinguished from the ones in the middle. Calculation of the PMs in the uppermost and lowest column sections are initialized in the destination regions, whereas calculation of the PMs in the middle section may be started from any point of the composition space.

Step 3: The PMs are investigated in pairs connected by junctions. Only those profiles are kept which satisfy the actual feasibility condition. Because purities are specified at the column end(s), this investigation is started at the uppermost and/or the lowest column sections, and is moved toward the other parts of the column.

Step 4: In the case of a batch rectifier or a batch stripper, the profiles in the last column section nearest the main

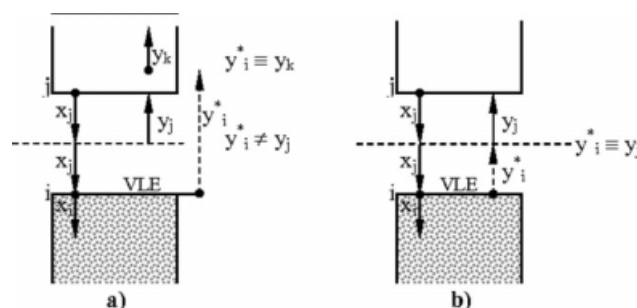


**Figure 4. Junction point of continuous column profiles without (a) and with (b) equality of the vapor compositions.**

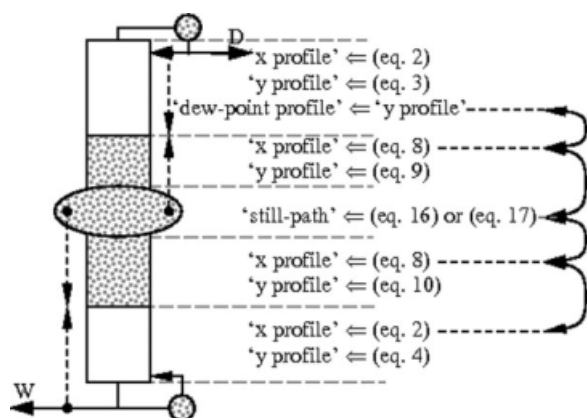


Figure 5. Necessary calculations for investigating the junction points of a MVC configuration.

vessel (either the reboiler or the reflux drum) determine the region of feasible vessel compositions. In the case of a MVC, the feasible region of the MV is given by the intersection of these two feasible regions.

Step 5: Integration of the still-path with the specified parameters ( $U_{MV}(0)$ ;  $x_{MV}(0)$ ;  $x_D$ ;  $x_W$ ;  $R$ ;  $S$ ;  $F$ ;  $z$ )

Step 6: The calculated still path is superposed on the feasible region and checked if and how long they overlap.

The separation is feasible with the fixed operation parameters if and only if the still-path overlaps the feasible region of the vessel.

### Application of the Generic Feasibility Study on the Production of Ethyl Acetate

In this section, the generic feasibility study on the production of ethyl acetate is presented in details step-by-step. No feed to the stripping part of the middle vessel column is considered in the feasibility study because any merit of applying such a feed can be excluded by considering the studied reaction. The feasibility of the process is studied with both infinite and finite reflux and reboil ratios. Because the same configurations are found feasible in both cases, the first four steps are presented with total reflux and reboil only, but the last three ones are discussed with finite reflux and reboil ratios.

#### Step 0: Parameters

The reaction in the studied system and its equilibrium constant expressed in concentration<sup>9</sup> are shown by Eqs. 18 and 19.



$$K = \frac{[\text{EtOAc}] \cdot [\text{H}_2\text{O}]}{[\text{EtOH}] \cdot [\text{AcOH}]} = 3.943 \quad (19)$$

The reaction equilibrium constant ( $K$ ) does not change with the temperature in the studied temperature range. The vapor-liquid equilibrium is modeled with NRTL equation. The model parameters presented in Table 4 are fitted with

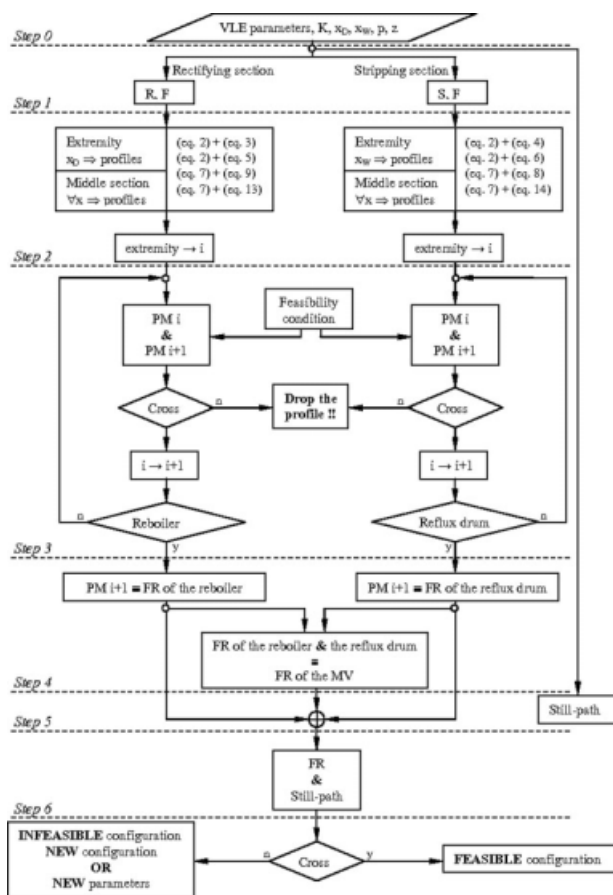


Figure 6. Strategy of the overall feasibility study.

ChemCAD<sup>®</sup> to UNIFAC model. The system contains three binary azeotropes and a ternary one, thus eight singular points are altogether presented in the system (Table 5).

#### Step 1: Specifications

The destination regions and the operation pressure are fixed for  $x_D \geq 0.95$ ,  $x_W \geq 0.95$ ,  $p = 1$  atm, respectively. The ratio of the feed flow rate to the vapor flow rate, the feed composition, the reflux ratio, and the reboil ratio, is varied. The feed is pure acetic acid in each case.

#### Step 2: Calculation of the profiles maps

Figures 7 and 8 show all the profiles maps necessary to study the feasibility with total reflux and total reboiling. The residue curves represent both the stripping and the rectifying

Table 4. VLE Model Parameters

Constituents	$g_{ij} - g_{ji}$	$g_{ii} - g_{ii}$	$\alpha_{ij}$
EtOH-AcOH	-293.6838	209.279	0.2992
EtOH-EtOAc	322.6216	306.4437	0.2987
EtOH-H <sub>2</sub> O	-109.6107	1332.3071	0.3031
AcOH-EtOAc	-436.9457	844.3039	0.3138
AcOH-H <sub>2</sub> O	-219.722	842.6148	0.2997
EtOAc-H <sub>2</sub> O	935.6937	2316.4112	0.4104

**Table 5. Singular Points of the System**

Constituents	Molar Compositions	Bubble Points (°)	Singular Points
EtOH-EtOAc-H <sub>2</sub> O	[0.191; 0.585; 0.224]	71.1	UN
EtOAc-H <sub>2</sub> O	[0.689; 0.311]	71.6	S
EtOH-EtOAc	[0.456; 0.544]	72.0	S
EtOAc		77.2	S
EtOH-H <sub>2</sub> O	[0.908; 0.092]	78.2	S
EtOH		78.3	S
H <sub>2</sub> O		100	S
AcOH		117.9	SN

profiles without product withdrawal both in the nonreactive (Figure 7a) and the reactive cases (Figure 7b).

There are eight singular points in the nonreactive residue curve map (Table 5). The AcOH vertex is the only stable node (SN), and the ternary azeotrope is the only unstable node (UN); thus, the whole tetrahedron forms a single distillation region. EtOAc and H<sub>2</sub>O are saddle points (S); thus, they cannot be produced without extractive sections.

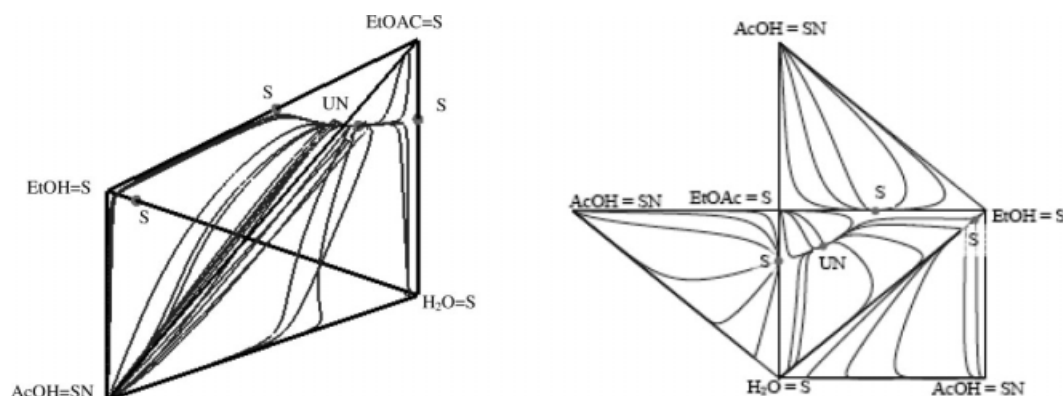
The reactive residue curves are presented in the transformed space (Figure 7b). Because there is no inert component in the system, the transformed domain is a rectangle.

No side of the rectangle is reactive; thus, the presence of the reaction can be neglected near to any side. The reactive residue curves map contains six singular points. Because of the reaction, the ternary azeotrope and the binary EtOAc-H<sub>2</sub>O azeotrope are not present. There are two stable nodes, denoted by SN (vertices AcOH and EtOH), and one unstable node, denoted by UN, (EtOAc-EtOH binary azeotrope) in this case; thus, there are two distillation regions separated by a separatrix connecting the EtOAc-EtOH and the EtOH-H<sub>2</sub>O binary azeotropes. Although the two main products (EtOAc and H<sub>2</sub>O) lie in the same distillation region, production of EtOAc is impossible in a reactive rectifier without extractive section because it remains a saddle point.

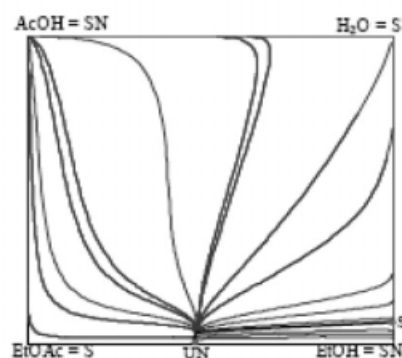
Because EtOAc always acts as a saddle point (denoted by S), extractive stages are needed to withdraw it in high purity.<sup>16</sup>

The extractive profiles maps are presented both in the nonreactive (Figures 8a, b) and in the reactive case (Figure 8c). The reactive profiles are shown in 2D transformed space only, whereas the nonreactive profiles are shown in 3D, and most of their singular points together with the residue curves, in unfolded faces.

The 2D representation is easier to understand but it is not sufficient for the nonreactive extractive profiles. There are only three stable nodes shown in Figure 8b, but there is a



a. Non-reactive residue curves. Left: 3D visualization. Right: unfolded faces.



b. Reactive residue curves shown in transformed co-ordinates

**Figure 7. Residue curves maps of the studied system.**

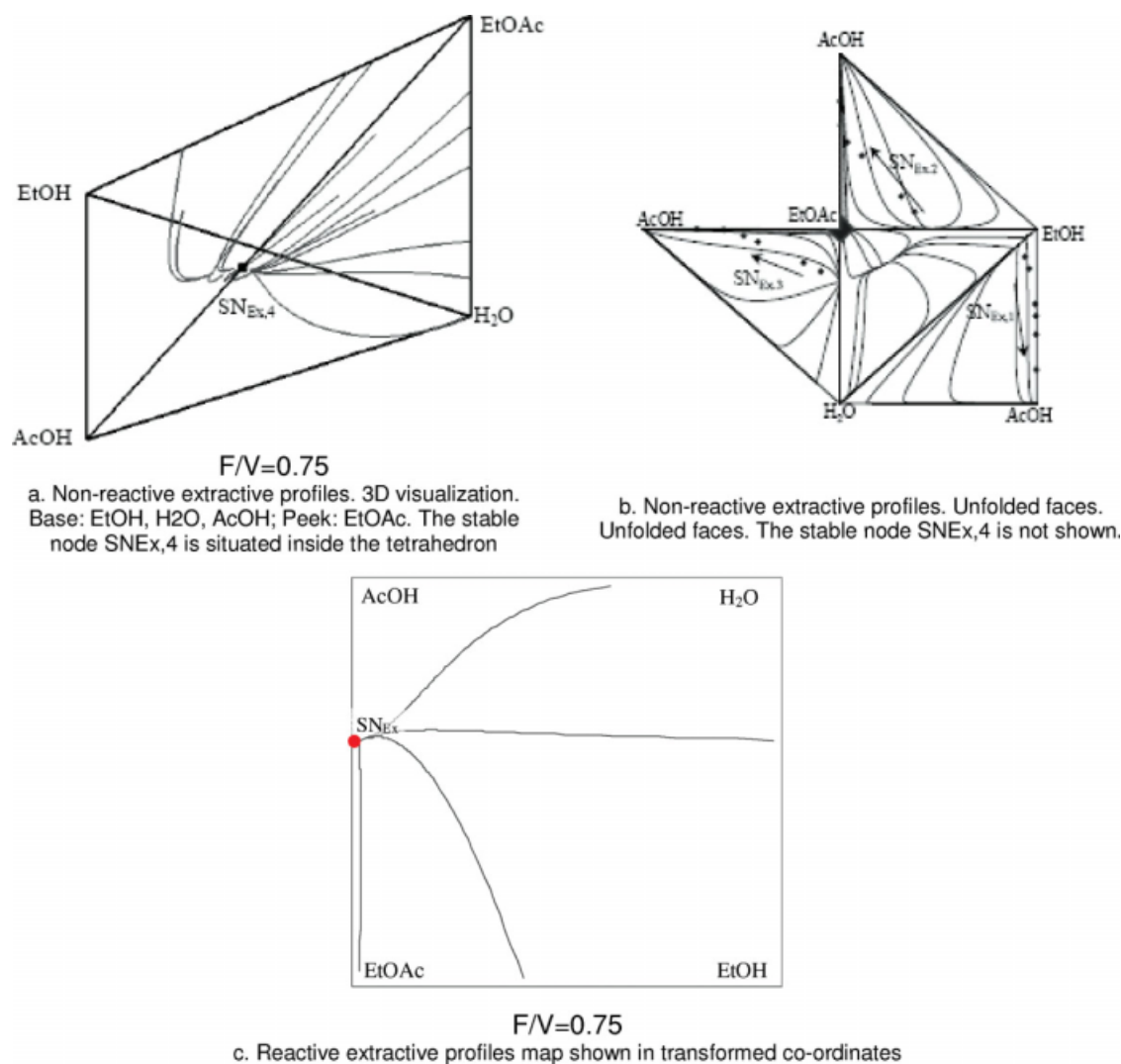


**Figure 8. Extractive profiles maps of the studied system at total reflux.**

[Color figure can be viewed in the online issue, which is available at [www.interscience.wiley.com](http://www.interscience.wiley.com).]

fourth one, as well, that moves inside the tetrahedron. Its presentation in 2D is difficult, but it is the most important stable node in viewpoint of feasibility. All the extractive profiles starting from any inside point of the tetrahedron, and not from any points of the four sides, converge to this stable node.

The four stable nodes unite in one if the feed ratio is higher than 0.75. At this feed ratio the stable node is situated in the EtOAc-AcOH side. This is the reason why only one SN is marked in Figure 8a.

### Step 3: Investigation of the calculated profiles

During the feasibility study, the middle vessel column is considered as a combination of a batch rectifier (above the middle vessel) and a batch stripper (below the middle vessel). The feasibility of these two parts is investigated separately.

*Batch Stripper.* As there is no feed considered in the stripping part of the middle vessel column, only three configurations (analogues to Figures 2a, c, d) can be distinguished and need to be investigated.

The bottom product is specified as 95% pure water, thus only those residue curves have to be studied which pass across the destination region assigned by this purity. According to section 2.3, the residue curves crossing the reactive space are considered as the ones making possible the production of pure water at the bottom with a reactive vessel. Figure 9 shows the curved reactive surface, and the bundle of nonreactive residue curves started from the destination region. All the nonreactive residue curves converge to the single UN in the EtOAc-EtOH-H<sub>2</sub>O face of the tetrahedron, without crossing the reactive surface. Because no stripping profile started from the destination region crosses the reactive surface, the batch nonreactive stripper with a reactive vessel cannot produce pure water.



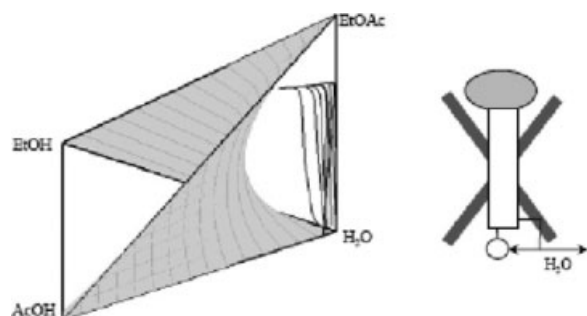


**Figure 9.** Investigation of the intersection of the non-reactive stripping profile and the reactive space with total reboil.

On the other hand, the reactive stripping profiles started from the destination region give a remarkably large feasible region (Figure 10), and the desired product can be withdrawn. The production of nearly pure water is possible in a fully reactive batch stripper.

Because one of the (necessary but not sufficient) feasibility conditions of the hybrid configuration analogous to Figure 2d is intersection of the nonreactive profile with the reactive space, that configuration is infeasible. (See the non-reactive stripping profiles in Figure 9.)

**Batch Rectifier.** As feed is also considered in the upper part of the column, all the eight configurations must be investigated. The top product is specified as 95% pure EtOAc. To satisfy the feasibility condition, the intersection of a dew point profile ( $x^*$  profile) of the corresponding residue curves started from the destination region and of the reactive space is examined (Figure 11). Because the  $x^*$  profiles run nearby the EtOAc-AcOH edge, the bundle of profiles intersecting the reactive surface is very narrow, the desired product can be produced with the configuration shown in Figure 2a but with a rather low recovery ratio only. Thus, application of this configuration is practically excluded.

The reactive residue curves started from the destination region (Figure 10) run also nearby the EtOAc-AcOH edge; thus, the fully reactive rectifier configuration (Figure 2c) is neither feasible. Because the edges are not reactive, there is no difference between the nonreactive rectifier and reactive one from the viewpoint of the feasibility study. Configuration of Figure 2d is also infeasible.

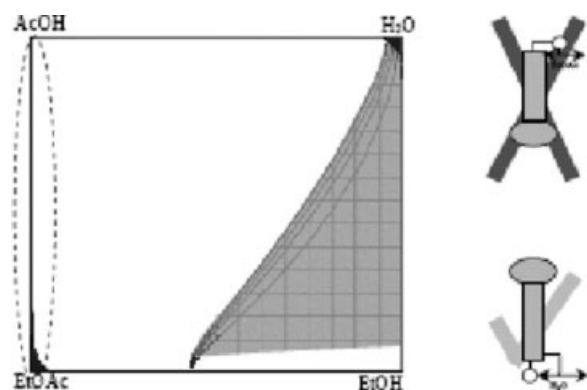


**Figure 10.** Feasible region of the reactive sections.

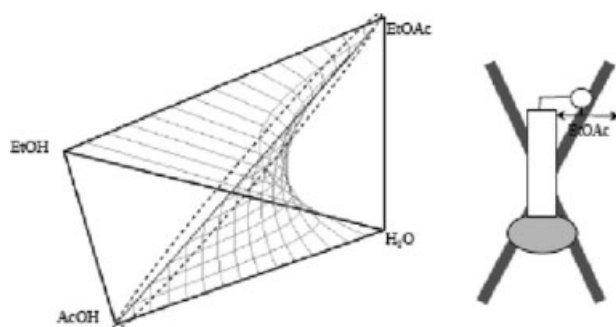


**Figure 11.** Possible intersection of the feasible region of the  $x^*$  profiles and the reactive space.

The nonreactive extractive profiles are shown in Figures 8a, b in Step 2. All the four stable nodes of the extractive profiles unite in one at  $F/V = 0.75$ ; thus, each extractive profile from the whole region runs into this point. The stable node is in the EtOAc-AcOH edge. The reactive and the non-reactive rectifier profiles run along the same edge. Because all the extractive profiles run to this common SN, the entire concentration region constitute the feasible region of the still, using total reflux and a feed ratio higher than 0.75. Therefore, the configuration shown in Figure 2b is feasible.

The situation is the same in the case of the reactive extractive profiles. SN is in the EtOAc-AcOH edge at feed ratio higher than 0.75 (Figure 8c); thus, the feasible region of the still is expanded for the entire reactive domain. The configuration presented in Figure 2e is also feasible.

All the hybrid configurations applying a continuous feed (Figures 2f–h) are also feasible because of the following reasons:

- The reactive rectifying profiles are the same as the non-reactive ones (the reaction is negligible along the binary mixture sides); thus, the configurations of Figures 2a, c, d are identical to the configurations of Figures 2e, f, h.
- The non reactive and the reactive extractive profiles run to the same SN, and both the reactive and the nonreactive extractive profiles expand the feasible region to the whole concentration domain. Thus, the configuration combining the reactive and nonreactive extractive sections (Figure 2g) is also feasible.

Because the shape of the different feasible regions (Figures 7 and 8) does not change with the applied reflux ratio, but only their size does, the same configurations are feasible with finite and infinite reflux ratios. Figure 12 shows all the feasible middle vessel configurations; they are feasible both with finite and infinite reflux and reboil ratios.

The last three steps of the feasibility study are presented with finite reflux and reboil ratios only.

#### **Step 4: Determination of the feasible reactive vessel region for the MVC configuration**

The feasible reactive middle vessel region is presented in the transformed 2D space because the reactive still-path is presented in the transformed space, as well.

A feasible region of the reactive vessel of a stripper is determined in studying the batch stripper in Step 3, and another feasible region of the reactive vessel of a rectifier is

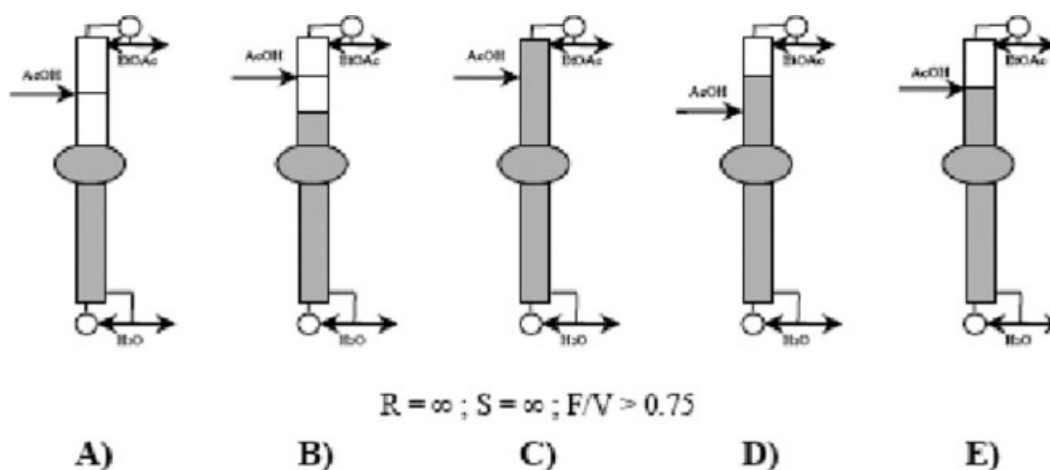


Figure 12. Feasible configurations of the MVC for producing pure EtOAc.

also determined in studying the batch rectifier in Step 3. The feasible region of the reactive middle vessel is the intersection of these two feasible regions because this vessel plays both roles. Because all the feasible configurations in Figure 12 incorporate the pure reactive stripper, the feasible reactive reflux drum region of the stripping part is formed by the reactive stripping profiles; these are shown in Figure 13.

For the rectifying part, the feasible reactive still region is given either by the feasible composition profiles right above the reactive still or by the intersection points of the dew point profiles and of the reactive space. According to Step3, the presence of an extractive section is necessary for producing EtOAc because otherwise the profiles run near the AcOH-EtOAc edge.

The feasible reactive middle vessel regions for the configurations shown in Figure 12 are considered below one-by-one.

In the case of the configuration in Figure 12A, the intersection points of the reactive surface and of the dew-point

profiles calculated from the feasible nonreactive extractive profiles must be investigated. The small squares in Figure 14 mark some of these intersection points, and we can estimate the region of all the intersection points by their hull (a region bordered by dotted line). The common part of this region and the region covered by the feasible reactive stripping profiles constitutes the feasible reactive middle vessel region of the studied configuration; this region is shaded in the Figure 14.

Because the configurations shown in Figures 12C–E, are identical in the viewpoint of feasibility, one figure is enough to find the feasible reactive middle vessel region of all these three configurations. In these cases, the region of the feasible reactive extractive profiles must be investigated. All those extractive profiles are feasible that end at or cross the AcOH-EtOAc side.

Figure 15 shows three reactive extractive profiles maps with different AcOH feed ratios. There is a feed ratio range that makes the separation feasible because the reactive extractive profiles reach the EtOAc-AcOH side. The feed ratio 0.75 is inside this range; 0.5 and 1.0 are outside this range. Although there are separatrices of the extractive profiles, all the profiles starting from a point of a feasible reactive stripping profile end in the AcOH-EtOAc side; thus, the feasible reactive middle vessel region is the whole feasible reactive stripping profiles region (Figure 16).

In the case of the configuration shown in Figure 12B, the intersection of the reactive and nonreactive extractive profiles must be investigated. In this case, those reactive extractive profiles are feasible that begin from the dotted line bordered region shown in Figure 14, and end in the AcOH-EtOAc side. The common region of these feasible reactive extractive profiles and the feasible reactive stripping profiles is identical to that shown in Figure 14 (see Figure 17).

Regarding the three feasible reactive middle vessel regions together, the configurations shown in Figures 12C–E, are characterized with the largest feasible region. Based solely on this information, one might choose any of these configurations. However, the last two steps must also be performed before one makes a final decision.

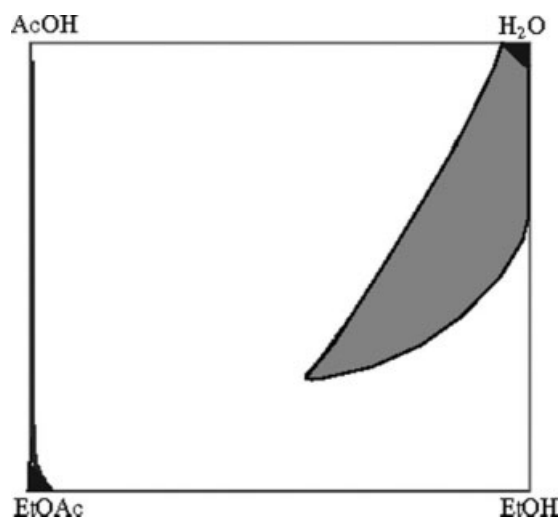


Figure 13. Reactive stripping and rectifying profiles at  $R = 10$  and  $S = 10$ .

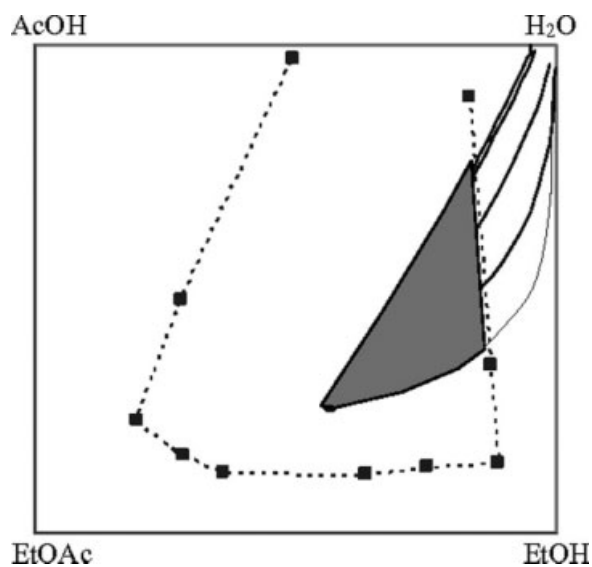


Figure 14. Feasible reactive middle vessel region of the configuration shown in Figure 12A.

However, preferable these configurations could be, none of them provides us with complete conversion of EtOH because none of the feasible reactive middle vessel regions reaches the binary AcOH-EtOAc side or the binary AcOH-H<sub>2</sub>O side.

#### Steps 5–6: Investigation of the still path and feasible region of the reactive vessel

To integrate the still-path, the initial composition of the middle vessel and the production ratio ( $D/W$ ) must be specified. Although it is not detailed above, the profile maps are calculated at several combinations of  $R$ ,  $S$ , and  $F/V$ , and proper value ranges are determined. Thus, we apply  $R = 10$ ,  $S = 10$ , and  $F/V = 0.75$  in the calculations shown below.

The initial composition is supposed to be in the feasible region along a straight line connecting the vertices of the pure reactants. The production ratio is varied to investigate the evolution of the still-path (Figure 18). The slope of the still-path changes with the production ratio, but converges to a limit slope at about  $D/W = 5$ .

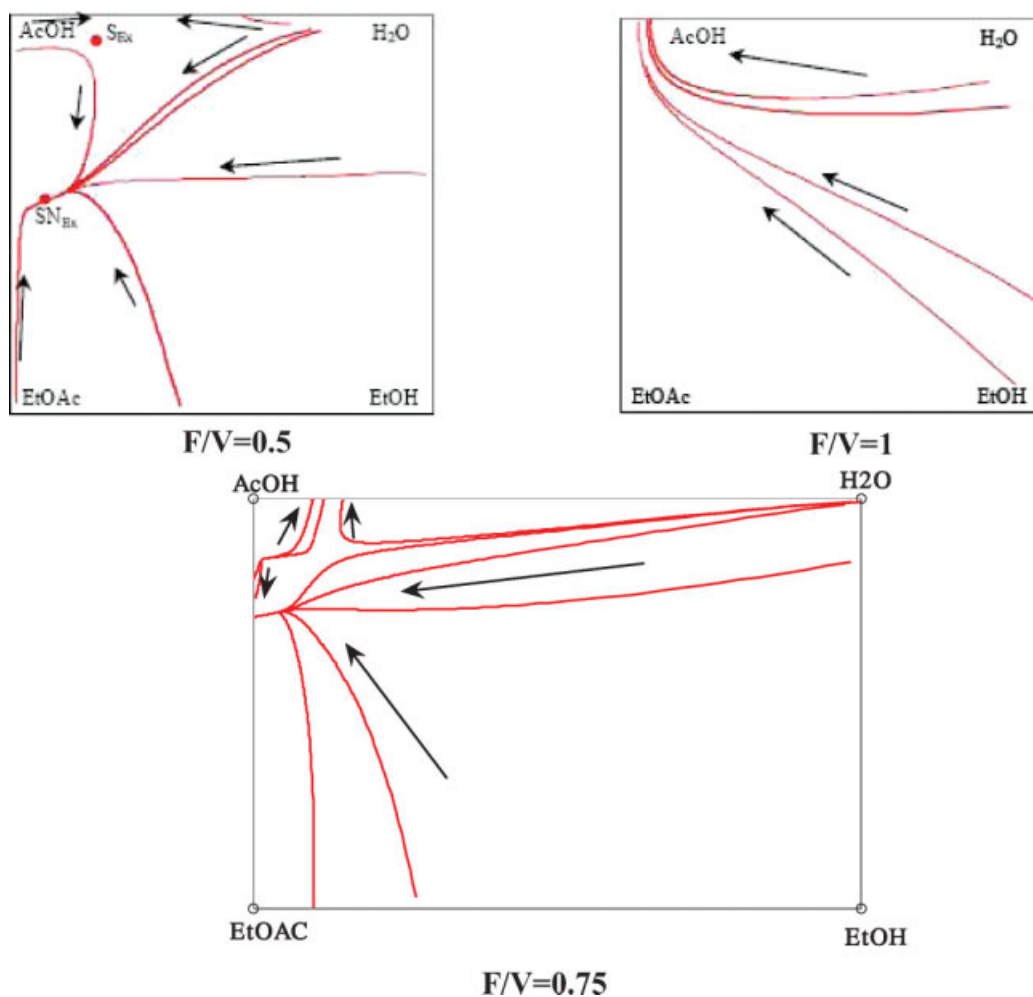


Figure 15. Reactive extractive profiles, at  $R = 10$ .

The reactive extractive profiles reach the EtOAc–AcOH side if the feed ration is about 0.75. [Color figure can be viewed in the online issue, which is available at [www.interscience.wiley.com](http://www.interscience.wiley.com).]

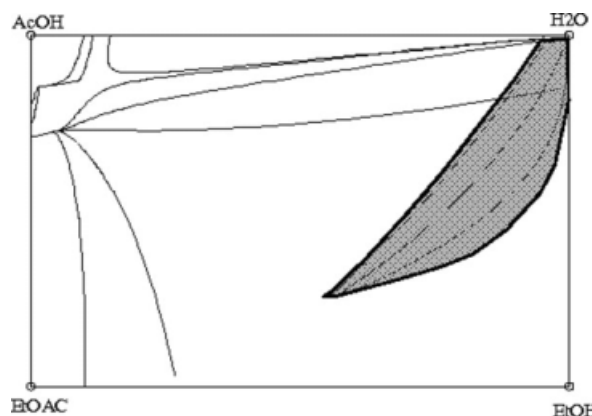


Figure 16. Feasible reactive middle vessel region of the configuration in the Figures 12C–E.

Although the feasible reactive middle vessel region is larger for the configurations shown in Figures 12C–E than for the others, all the five configurations are identical from the viewpoint of feasibility. In each case the reactive stripping profiles zone determines the end point of the production. Once the still-path crosses the border of the stripping profiles zone, further producing both desired products simultaneously is impossible.

## Conclusions

A new graphical feasibility method is developed to investigate batch reactive distillation processes in middle vessel column. The suggested methodology can deal with fully reactive, fully nonreactive, and complex, column sections with a reactive vessel. The model equations of reactive sections and still path are developed using transformed component flow rates in accordance with the model equations of Lelkes et al.<sup>4</sup> Use of the new formulation is suggested to describe the composition profiles in the reactive sections. Its application has made possible to develop a generic feasibility methodology containing the same model equations independently of the presence or absence of reaction. By combining the re-

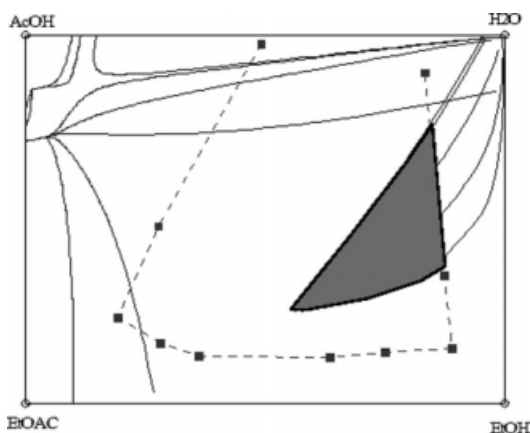


Figure 17. Feasible reactive middle vessel region of the configuration in the Figure 12B.

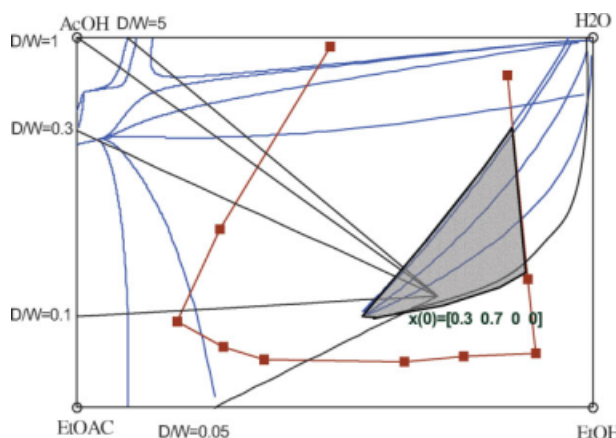


Figure 18. Still paths calculated with different production ratios.

[Color figure can be viewed in the online issue, which is available at [www.interscience.wiley.com](http://www.interscience.wiley.com).]

active and nonreactive models, not only the fully reactive and fully nonreactive but also hybrid configurations can be studied. Feasibility criteria related to the hybrid configurations are also presented.

Application of the new methodology is demonstrated on the production of ethyl acetate in batch reactive distillation. Five configurations are found feasible. Pure EtOAc is produced as distillate, and H<sub>2</sub>O is produced as bottom product. In each case, continuous feeding of AcOH is necessary to break the EtOH–EtOAc azeotrope. The five feasible configurations are found identical from the viewpoint of feasibility. To find the best configuration, optimized variants ought to be compared, but optimization is not the aim of this publication.

Because our method remains to be of graphical nature, the feasibility study of a system having more than four components might be difficult because the visualization in more than 3D is impossible. This methodology, with applying some modifications, can be used to continuous processes, as well. Moreover, the feasibility methodology can be extended for multireaction systems, as well, by defining a new transformation.

## Acknowledgments

This work was supported by the Hungarian and French Governments, and by the Hungarian National Research Fund (OTKA) K062099, F046282, and T037191.

## Notation

- $D$  = distillate flowrate
- $d$  = distillate component flowrate
- $F$  = feed flowrate
- $f$  = feed component flowrate
- $h$  = dimensionless height
- $K$  = equilibrium constant expressed in concentration
- $l$  = liquid component flowrate
- $L$  = molar liquid flowrate
- $U$  = molar holdup in the still
- $V$  = molar vapor flowrate
- $W$  = molar flow rate of bottom product
- $w$  = component flowrate of bottom product



$v$  = vapor component flowrate  
 $x$  = liquid composition  
 $X$  = transformed composition  
 $y$  = vapor composition  
 $y^*$  = vapor composition in equilibrium with  $x$   
 $z$  = feed composition  
 $\nu$  = stoichiometric coefficient  
 $\xi$  = reaction coordinate

### Subscripts and superscripts

$D$  = distillate  
 $i$  =  $i$ th component  
 MV = middle vessel  
 nc = number of components  
 ref = reference component  
 $T$  = total  
 $W$  = bottom product  
 $\sim$  = transformed variable

### Literature Cited

- Doherty MF, Buzad G. Reactive distillation by design. *Trans I Chem E*. 1992;70:448–458.
- Sundmacher K, Kienle A, editors. *Reactive Distillation*. Weinheim: Wiley-VCH, 2002.
- Almeida-Rivera CP, Swinkels PLJ, Grievink J. Designing reactive distillation processes: present and future. *Comp Chem Eng*. 2004;28:1997–2020.
- Lelkes Z, Lang P, Benadda B, Moszkowicz P. Feasibility of extractive distillation in a batch rectifier. *AIChE J*. 1998;44:810–822.
- Safrit BT, Westerberg AW, Diwekar U, Wahnschafft OM. Extending continuous conventional extractive distillation feasibility insights to batch distillation. *Ind Eng Chem Res*. 1995;34:3257–3264.
- Laroche L, Bekiaris N, Andersen HW, Morari M. Homogeneous azeotropic distillation. Comparing entrainers. *Can J Chem Eng*. 1991;69:1302–1319.
- Guo Z, Ghufuran M, Lee JW. Feasibility products in batch reactive distillation. *AIChE J*. 2003;49:3161–3172.
- Guo Z, Lee JW. Feasibility products in batch reactive extractive distillation. *AIChE J*. 2004;50:1484–1492.
- Espinosa J. On the integration of reaction and separation in a batch extractive distillation column with a middle vessel. *Ind Eng Chem Res*. 2002;41:3657–3666.
- Pisarenko YA, Cardona CA, Danilov RY, Serafimov LA. *Design Method of Optimal Technological Flow Sheets for Reactive Distillation Processes*. Montpellier, France: ECCE2, 1999.
- Espinosa J, Aguirre P, Perez A. Product composition regions of single-feed reactive distillation columns: mixtures containing inerts. *Ind Eng Chem Res*. 1995;34:853–861.
- Espinosa J, Aguirre P, Perez A. Some aspects in the design of multi-component reactive distillation with a reacting core: mixture containing inerts. *Ind Eng Chem Res*. 1996;35:4537–4549.
- Groemping M, Dragomir RM, Jobson M. Conceptual design of reactive distillation columns using stage composition lines. *Chem Eng Proc*. 2004;43:369–382.
- Dragomir RM, Jobson M. Conceptual design of single-feed hybrid reactive distillation columns. *Chem Eng Sci*. 2005;60:4377–4395.
- Chin J, Kattukaran HJ, Lee JW. Generalized feasibility evaluation of equilibrated quaternary reactive distillation, systems. *Ind Eng Chem Res*. 2004;43:7092–7102.
- Bessling B, Schembecker G, Simmrock KH. Design of processes with reactive distillation line diagrams. *Ind Eng Chem Res*. 1997;36:3032–3042.
- Boneta J, Thery R, Meyer X, Meyer M, Reneaume J-M, Galan M-I, Costa J. *Infinite/Infinite Analysis as a Tool for an Early Oriented Synthesis of a Reactive Pressure Swing Process*. Barcelona, Spain: ESCAPE-15, 2005.
- Varga V, Frits ER, Gerbaud V, Fonyo Z, Joulia X, Lelkes Z, Rev E. *Separation of Azeotropes in Batch Extractive Stripper with Intermediate Entrainer*. Garmisch-Partenkirchen, Germany: ESCAPE-16 & PSE, 2006.
- Low K, Sorensen E. Optimal operation of extractive distillation in different batch configurations. *AIChE J*. 2002;48:1034–1050.
- Rodríguez DI, Gerbaud V, Joulia X. Feasibility of heterogeneous batch distillation processes. *AIChE J*. 2002;48:1168–1178.
- Modla G, Lang P, Kotai B, Molnar K. Batch heteroazeotropic rectification of a low mixture under continuous entrainer feeding. *AIChE J*. 2003;49:2533–2552.
- Donis IR, Esquijarosa JA, Gerbaud V, Joulia X. Heterogeneous batch-extractive distillation of minimum boiling azeotropic mixtures. *AIChE J*. 2003;49:3074–3083.
- Chin J, Lee JW. Rapid generation of composition profiles for reactive and extractive cascades. *AIChE J*. 2005;51:922–930.
- Chin J, Lee JW, Choe J. Feasible products in complex batch reactive distillation. *AIChE J*. 2006;52:1790–1805.

### Appendix A: Derivation of the Reactive Profile Equations

The component balance around the  $n$ th theoretical reactive tray, counted downward, can be written by (A1) applying the reaction coordinate for the reactive term.

$$l_{n,i} + v_{n,i}^* = l_{n-1,i} + v_{n+1,i} + v_i \cdot \dot{\xi} \quad (\text{A1})$$

The reaction term in (A1) can be eliminated with the application of a reference component as is shown in (A2)

$$\dot{\xi} = \frac{(l_{n,\text{ref}} - l_{n-1,\text{ref}}) + (v_{n,\text{ref}}^* - v_{n+1,\text{ref}})}{v_{\text{ref}}} \quad (\text{A2})$$

By substitution and rearrangement, we obtain

$$l_{n,i} + v_{n,i}^* = l_{n-1,i} + v_{n+1,i} + \frac{v_i}{v_{\text{ref}}} \cdot \left[ (l_{n,\text{ref}} - l_{n-1,\text{ref}}) + (v_{n,\text{ref}}^* - v_{n+1,\text{ref}}) \right] \quad (\text{A3})$$

$$\begin{aligned} & \left( l_{n,i} - \frac{v_i}{v_{\text{ref}}} \cdot l_{n,\text{ref}} \right) - \left( l_{n-1,i} - \frac{v_i}{v_{\text{ref}}} \cdot l_{n-1,\text{ref}} \right) \\ &= \left( v_{n+1,i} - \frac{v_i}{v_{\text{ref}}} \cdot v_{n+1,\text{ref}} \right) - \left( v_{n,i}^* - \frac{v_i}{v_{\text{ref}}} \cdot v_{n,\text{ref}}^* \right) \end{aligned} \quad (\text{A4})$$

Because the terms in the brackets are analogous to each other, the transformed variables presented by (A5) can be introduced to simplify the relationship and be written as (A6).

$$\tilde{l}_{n,i} = l_{n,i} - \frac{v_i}{v_{\text{ref}}} \cdot l_{n,\text{ref}} \quad \text{and} \quad \tilde{v}_{n+1,i} = v_{n+1,i} - \frac{v_i}{v_{\text{ref}}} \cdot v_{n+1,\text{ref}} \quad (\text{A5})$$

$$\tilde{l}_{n,i} - \tilde{l}_{n-1,i} = \tilde{v}_{n+1,i} - \tilde{v}_{n,i}^* \quad (\text{A6})$$

We stop expanding the Taylor series of component flowrate at the first degree; and express the differential according to (A7). Because the transformation (A5) is linear, the differential remains the same for the transformed variables (A8).

$$l_{n,i} = l_{n-1,i} + \left. \frac{dl_i}{dh} \right|_{h=n-1} \cdot (n - (n - 1)) \Rightarrow \frac{dl_i}{dh} = l_{n,i} - l_{n-1,i} \quad (\text{A7})$$

$$\frac{d\tilde{l}}{dh} = \tilde{l}_{n,i} - \tilde{l}_{n-1,i} \quad (\text{A8})$$

The left-hand side of Eq. A6 is equal to the right-hand side of Eq. A8. These two equations are combined to obtain

the basic model equation describing the evaluation of the reactive profile in the column.

$$\frac{d\tilde{l}_i}{dh} = \tilde{v}_{n+1,i} - \tilde{v}_{n,i}^*$$

The operation line in a reactive rectifying section is written by (A9)

$$l_{n,i} + d_i = v_{n+1,i} + v_i \sum_{\text{rectifying section}} \dot{\xi} \quad (\text{A9})$$

The reaction term can be eliminated with the help of the reference component. Performing the same derivation as before, the transformed variables of (A5) can be applied, and the reactive operation line can be written as

$$\tilde{v}_{n+1,i} = \tilde{l}_{n,i} + \tilde{d}_i$$

## Appendix B: Derivation of the Equivalence

Here, we show that the mole fractions calculated with the new transformed variables are identical to the ones published by Doherty and Buzad.<sup>1</sup> The derivation is presented only for the liquid compositions, but it can be applied to the vapor compositions, as well.

Our transformed variables for the liquid molar flow rates are written by Eq. 7

$$\tilde{l}_i = l_i - \frac{v_i}{v_{\text{ref}}} \cdot l_{\text{ref}} \quad (\text{B1})$$

The transformed mole fractions of a given flow can be calculated in analogy with Eq. 11

$$\tilde{x}_i = \frac{\tilde{l}_i}{\sum_{j=1}^{nc} \tilde{l}_j} = \frac{l_i - \frac{v_i}{v_{\text{ref}}} \cdot l_{\text{ref}}}{\sum_{j=1}^{nc} \left( l_j - \frac{v_j}{v_{\text{ref}}} \cdot l_{\text{ref}} \right)} \quad (\text{B2})$$

Since  $\sum_i (\alpha_i + \beta \cdot \gamma_i) \equiv \sum_i \alpha_i + \beta \cdot \sum_i \gamma_i$  and  $\sum_{j=1}^{nc} v_j \equiv v_T$

$$\begin{aligned} \tilde{x}_i &= \frac{l_i - \frac{v_i}{v_{\text{ref}}} \cdot l_{\text{ref}}}{\sum_{j=1}^{nc} l_j - \frac{v_T}{v_{\text{ref}}} \cdot l_{\text{ref}}} = \frac{l_i - \frac{v_i}{v_{\text{ref}}} \cdot l_{\text{ref}}}{\sum_{j=1}^{nc} l_j} \cdot \frac{\sum_{j=1}^{nc} l_j}{\sum_{j=1}^{nc} l_j - \frac{v_T}{v_{\text{ref}}} \cdot l_{\text{ref}}} \\ &= \frac{x_i - \frac{v_i}{v_{\text{ref}}} \cdot x_{\text{ref}}}{1 - \frac{v_T}{v_{\text{ref}}} \cdot x_{\text{ref}}} \quad (\text{B3}) \end{aligned}$$

The suggested transformation by Doherty and Buzad<sup>1</sup> is written as  $x_i = \frac{x_i - \frac{v_i}{v_{\text{ref}}} \cdot x_{\text{ref}}}{1 - \frac{v_T}{v_{\text{ref}}} \cdot x_{\text{ref}}}$ , thus

$$\tilde{x}_i = \frac{\tilde{l}_i}{\sum_{j=1}^{nc} \tilde{l}_j} \equiv x_i$$

## Appendix C: Derivation of the Reactive Still Path Equation

The still-path equation for a batch middle vessel column configuration without any additional feed is derived here. The differential component balance of the middle vessel accounts for the composition change due to product withdrawals and the reaction in the whole column. The right

hand side of the differential Eq. C1 refers to these factors.

$$\frac{d(U_{\text{MV}} x_{\text{MV},i})}{dt} = -D x_{D,i} - W x_{W,i} + v_i \sum_{\text{column}} \dot{\xi} \quad (\text{C1})$$

The reaction term can be eliminated with the application of a reference component.

$$\sum_{\text{column}} \dot{\xi} = \frac{D x_{D,\text{ref}} + W x_{W,\text{ref}} + \frac{d(U_{\text{MV}} x_{\text{MV},\text{ref}})}{dt}}{v_{\text{ref}}} \quad (\text{C2})$$

$$\begin{aligned} \frac{d(U_{\text{MV}} x_{\text{MV},i})}{dt} - \frac{v_i}{v_{\text{ref}}} \frac{d(U_{\text{MV}} x_{\text{MV},\text{ref}})}{dt} &= -D \left( x_{D,i} - \frac{v_i}{v_{\text{ref}}} x_{D,\text{ref}} \right) \\ &\quad - W \left( x_{W,i} - \frac{v_i}{v_{\text{ref}}} x_{W,\text{ref}} \right) \quad (\text{C3}) \end{aligned}$$

The right hand side of the equation can be written in a simpler form with the help of the transformed variables suggested by Sundmacher and Kienle,<sup>2</sup> Espinosa et al.,<sup>12</sup> and Doherty and Buzad<sup>1</sup>.

$$\begin{aligned} \frac{d(U_{\text{MV}} x_{\text{MV},i})}{dt} - \frac{v_i}{v_{\text{ref}}} \frac{d(U_{\text{MV}} x_{\text{MV},\text{ref}})}{dt} &= -D \left( 1 - \frac{v_T}{v_{\text{ref}}} x_{D,\text{ref}} \right) \frac{x_{D,i} - \frac{v_i}{v_{\text{ref}}} x_{D,\text{ref}}}{1 - \frac{v_T}{v_{\text{ref}}} x_{D,\text{ref}}} \\ &\quad - W \left( 1 - \frac{v_T}{v_{\text{ref}}} x_{W,\text{ref}} \right) \frac{x_{W,i} - \frac{v_i}{v_{\text{ref}}} x_{W,\text{ref}}}{1 - \frac{v_T}{v_{\text{ref}}} x_{W,\text{ref}}} \quad (\text{C4}) \end{aligned}$$

$$\frac{d(U_{\text{MV}} x_{\text{MV},i})}{dt} - \frac{v_i}{v_{\text{ref}}} \frac{d(U_{\text{MV}} x_{\text{MV},\text{ref}})}{dt} = -\hat{D} x_{D,i} - \hat{W} x_{W,i} \quad (\text{C5})$$

The transformed mole fraction in the left hand side of the equation must appear in differential form; thus, only this side of the equation is modified further:

$$\begin{aligned} \frac{d(U_{\text{MV}} x_{\text{MV},i})}{dt} - \frac{v_i}{v_{\text{ref}}} \frac{d(U_{\text{MV}} x_{\text{MV},\text{ref}})}{dt} &= U_{\text{MV}} \frac{dx_{\text{MV},i}}{dt} \\ &\quad + x_{\text{MV},i} \frac{dU_{\text{MV}}}{dt} - U_{\text{MV}} \frac{v_i}{v_{\text{ref}}} \frac{dx_{\text{MV},\text{ref}}}{dt} - \frac{v_i}{v_{\text{ref}}} x_{\text{MV},\text{ref}} \frac{dU_{\text{MV}}}{dt} \quad (\text{C6}) \end{aligned}$$

$$\begin{aligned} \frac{d(U_{\text{MV}} x_{\text{MV},i})}{dt} - \frac{v_i}{v_{\text{ref}}} \frac{d(U_{\text{MV}} x_{\text{MV},\text{ref}})}{dt} &= U_{\text{MV}} \left( \frac{dx_{\text{MV},i}}{dt} - \frac{v_i}{v_{\text{ref}}} \frac{dx_{\text{MV},\text{ref}}}{dt} \right) \\ &\quad + x_{\text{MV},i} \left( 1 - \frac{v_T}{v_{\text{ref}}} x_{\text{MV},\text{ref}} \right) \frac{dU_{\text{MV}}}{dt} \quad (\text{C7}) \end{aligned}$$

Relation (C7) cannot be simplified further, but the term in the first bracket on the right side can be derived from the differential form of the reactive mole fraction.

$$\frac{dx_{\text{MV},i}}{dt} = \frac{d \left( \frac{x_{\text{MV},i} - \frac{v_i}{v_{\text{ref}}} x_{\text{MV},\text{ref}}}{1 - \frac{v_T}{v_{\text{ref}}} x_{\text{MV},\text{ref}}} \right)}{dt} \quad (\text{C8})$$

$$\frac{dx_{MV,i}}{dt} = \frac{\left(1 - \frac{v_T}{v_{ref}} x_{MV,ref}\right) \left(\frac{dx_{MV,i}}{dt} - \frac{v_i}{v_{ref}} \frac{dx_{MV,ref}}{dt}\right) - \left(x_{MV,i} - \frac{v_i}{v_{ref}} x_{MV,ref}\right) \left(-\frac{v_T}{v_{ref}} \frac{dx_{MV,ref}}{dt}\right)}{\left(1 - \frac{v_T}{v_{ref}} x_{MV,ref}\right)^2} \quad (C9)$$

$$\begin{aligned} \frac{dx_{MV,i}}{dt} - \frac{v_i}{v_{ref}} \frac{dx_{MV,ref}}{dt} &= \frac{\frac{dx_{MV,i}}{dt} \left(1 - \frac{v_T}{v_{ref}} x_{MV,ref}\right)^2 + \left(x_{MV,i} - \frac{v_i}{v_{ref}} x_{MV,ref}\right) \left(-\frac{v_T}{v_{ref}} \frac{dx_{MV,ref}}{dt}\right)}{\left(1 - \frac{v_T}{v_{ref}} x_{MV,ref}\right)} \\ &= \frac{dx_{MV,i}}{dt} \left(1 - \frac{v_T}{v_{ref}} x_{MV,ref}\right) + \left(x_{MV,i} - \frac{v_i}{v_{ref}} x_{MV,ref}\right) \left(-\frac{v_T}{v_{ref}} \frac{dx_{MV,ref}}{dt}\right) \end{aligned} \quad (C10)$$

$$\begin{aligned} \frac{dx_{MV,i}}{dt} - \frac{v_i}{v_{ref}} \frac{dx_{MV,ref}}{dt} &= \frac{dx_{MV,i}}{dt} \left(1 - \frac{v_T}{v_{ref}} x_{MV,ref}\right) \\ &\quad - X_{MV,i} \frac{v_T}{v_{ref}} \frac{dx_{MV,ref}}{dt} \end{aligned} \quad (C11)$$

Relation (C11) is now substituted into the term of the first bracket in the right hand side of (C7).

$$\begin{aligned} \frac{d(U_{MV} x_{MV,i})}{dt} - \frac{v_i}{v_{ref}} \frac{d(U_{MV} x_{MV,ref})}{dt} &= \hat{U}_{MV} \frac{dx_{MV,i}}{dt} + x_{MV,i} \left(1 - \frac{v_T}{v_{ref}} x_{MV,ref}\right) \frac{dU_{MV}}{dt} \\ &\quad - U_{MV} X_{MV,i} \frac{v_T}{v_{ref}} \frac{dx_{MV,ref}}{dt} \end{aligned} \quad (C12)$$

(C5) and (C12) have the same term in the left hand side; thus, they are equal.

$$\begin{aligned} \hat{U}_{MV} \frac{dx_{MV,i}}{dt} &= -X_{MV,i} \left(1 - \frac{v_T}{v_{ref}} x_{MV,ref}\right) \frac{dU_{MV}}{dt} \\ &\quad + U_{MV} X_{MV,i} \frac{v_T}{v_{ref}} \frac{dx_{MV,ref}}{dt} - \hat{D} X_{D,i} - \hat{W} X_{W,i} \end{aligned} \quad (C13)$$

The mass balance of the MV, in analogy to the component balance (see C1), is given by

$$\frac{dU_{MV}}{dt} = -D - W + v_T \sum_{\text{column}} \dot{\xi} \quad (C14)$$

Substitution of (C14) to (C13) gives the final general form in the presence of one instantaneously equilibrium limited reaction.

$$\begin{aligned} \hat{U}_{MV} \frac{dx_{MV,i}}{dt} &= \hat{D} \left( X_{MV,i} \frac{1 - \frac{v_T}{v_{ref}} x_{MV,ref}}{1 - \frac{v_T}{v_{ref}} x_{D,ref}} - X_{D,i} \right) \\ &\quad + \hat{W} \left( X_{MV,i} \frac{1 - \frac{v_T}{v_{ref}} x_{MV,ref}}{1 - \frac{v_T}{v_{ref}} x_{W,ref}} - X_{W,i} \right) \\ &\quad - X_{MV,i} \left(1 - \frac{v_T}{v_{ref}} x_{MV,ref}\right) v_T \sum_{\text{oszlop}} \dot{\xi} + U_{MV} X_{MV,i} \frac{v_T}{v_{ref}} \frac{dx_{MV,ref}}{dt} \end{aligned}$$

The general equation cannot be solved graphically, but its form is much simpler in the case of equimolar reactions, namely when  $v_T = 0$ . In the case of an equimolar reaction, the reactive flow rates are equal to the nonreactive ones; therefore,  $\hat{U}_{MV} = U_{MV}$ ,  $\hat{D} = D$ , and  $\hat{W} = W$ . In this case, application of the dimensionless time  $(d\tau = \frac{1}{U_{MV}} dt)$  further simplifies the equation:

$$\frac{dx_{MV,i}}{d\tau} = D(X_{MV,i} - X_{D,i}) + W(X_{MV,i} - X_{W,i})$$

*Manuscript received Feb. 19, 2008, revision received Jul. 4, 2008, and final revision received Oct. 6, 2008.*